

2002

## Improvement of SOI microdosimeter performance using pulse-shape discrimination techniques

I. Cornelius

*University of Wollongong*

Anatoly B. Rosenfeld

*University of Wollongong, [anatoly@uow.edu.au](mailto:anatoly@uow.edu.au)*

R. Siegele

*ANSTO, Australia*

D. D. Cohen

*ANSTO, Australia*

Follow this and additional works at: <https://ro.uow.edu.au/engpapers>



Part of the [Engineering Commons](#)

<https://ro.uow.edu.au/engpapers/6>

---

### Recommended Citation

Cornelius, I.; Rosenfeld, Anatoly B.; Siegele, R.; and Cohen, D. D.: Improvement of SOI microdosimeter performance using pulse-shape discrimination techniques 2002.  
<https://ro.uow.edu.au/engpapers/6>

# Improvement of SOI Microdosimeter Performance Using Pulse-Shape Discrimination Techniques

Iwan Cornelius, *Student Member, IEEE*, Anatoly Rosenfeld, *Senior Member, IEEE*, Rainer Siegele, and David D. Cohen

**Abstract**—The timing properties of a silicon-on-insulator microdosimeter for medical and space applications have been studied using an ion microprobe. These measurements were used with a pulse-shape discrimination technique to render the microdosimeter insensitive to ion strikes outside the ideal sensitive volume. These improvements have resulted in a microdosimeter with a cubic sensitive volume with dimensions  $10 \times 10 \times 10 \mu\text{m}^3$ , a charge collection spectrum close to Gaussian for a monoenergetic source, and a decreased sensitivity to radiation damage.

**Index Terms**—Microdosimetry, pulse-shape discrimination.

## I. INTRODUCTION

MICRODOSIMETRY is used to study the radiobiological properties of densely ionizing radiations as encountered in hadron therapy and space environments [1]. To determine risk estimates, a spectrum of lineal energy values of the radiation field is measured. This spectrum is conventionally measured with a gas filled tissue equivalent proportional counter (TEPC), which registers energy deposition events in a simulated microscopic volume. The TEPC does, however, have several disadvantages as outlined in the literature [1], [2].

The creation of a solid-state microdosimeter to replace the TEPC for monitoring the radiation environment aboard spacecraft and in avionics is the topic of ongoing research. Different approaches based on FAMOS devices [3] and memory devices [4] have been proposed. Such microdosimeters should be reliable, radiation hard, and utilize data acquisition electronics suitable for on board application. The Centre for Medical Radiation Physics has been investigating a technique using microscopic arrays of reverse biased pn junctions. A prototype SOI microdosimeter was developed and measurements were conducted at boron neutron capture therapy [5], proton therapy [6], and fast neutron therapy [2] facilities. [2] provides a comparison between the TEPC and silicon microdosimeters, highlighting the cost, convenience, and accuracy of the instruments.

The SOI diode array is manufactured by Fujitsu on a bonded p-type SOI wafer of thickness 2, 5, or  $10 \mu\text{m}$ .  $n^+$  and  $p^+$  silicon regions are constructed with Arsenic and Boron implantations (see Fig. 2) at  $30 \text{ keV}$  at a fluence of  $5 \times 10^{15} \text{ cm}^{-2}$ . The impurity concentration of the p-type silicon is  $1.5 \times 10^{15} \text{ cm}^{-3}$ . All diodes in the array are connected in parallel and each pn junction

has an area of  $10 \times 10 \mu\text{m}^2$  (see Fig. 1). The total size of each diode cell is  $30 \times 30 \mu\text{m}^2$ . With  $120 \times 40$  diodes in a single device, the total array area is  $0.044 \text{ cm}^2$ . The microdosimeter is incorporated into a lucite probe for microdosimetry measurements in hadron therapy. The detector is connected to an AMPTEK A250 radiation-hard charge sensitive preamplifier in close proximity to reduce input capacitance. Noise is minimized by encapsulating the entire probe in aluminum shielding, which is then connected to the coaxial cable ground. This also ensures that the chip does not receive any light, which generates significant noise via surface photo generation. The microdosimeter collects charge generated by the traversal of an ion through the device's sensitive volume. The charge collected is proportional to the energy deposited, as it requires  $3.6 \text{ eV}$  to generate an electron hole pair in silicon. The output of the preamplifier is a voltage pulse with amplitude proportional to the energy deposited in the sensitive volume of the microdosimeter. The pulse height from each event is digitized and stored using a PC based multichannel analyzer (MCA). This spectrum is then converted to a lineal energy spectrum, from which the radiobiological effectiveness of the radiation field at the point of measurement may be estimated [1]. A detailed description of the device and readout electronics is given in [6].

To accurately measure the lineal energy spectrum the microdosimeter must possess a well defined charge collection volume (ideally the depletion region of the pn junction). This should be as close to spherical as possible (or more realistically for the case of silicon devices cubic) in order to minimize the variation of chord lengths through the device. It is also important for the microdosimeter to provide a spectrum of energy deposition events which is close to Gaussian for a monoenergetic ion beam. This removes the need to deconvolute the lineal energy spectrum from the measured spectrum. Previous studies were conducted using ion beam induced charge collection imaging (IBIC) with ion microprobes [7], [8] to quantify the charge collection properties of the SOI microdosimeter. The results of these studies showed that significant charge collection occurred for ion strikes outside the junction (the ideal sensitive volume) due to the diffusion of charge carriers. Consequently, the current microdosimeter design results in a poor spectral response due to incomplete charge collection, a dependence upon device overlayer, a strong angular dependence due to the ill defined sensitive volume and a sensitivity to radiation damage.

Pulse-shape discrimination techniques involve measurement of the timing properties of signals collected from radiation detectors. Considerable work has been performed in the field of particle identification (see [9]–[11] and references therein).

Manuscript received July 16, 2002; revised September 25, 2002.

I. Cornelius and A. Rosenfeld are with the Centre for Medical Radiation Physics, University of Wollongong, Wollongong, NSW 2522, Australia (e-mail: ic02@uow.edu.au).

R. Siegele and D. Cohen are with Physics Division, Australian Nuclear Science and Technology Organization, Lucas Heights, NSW 2234, Australia.

Digital Object Identifier 10.1109/TNS.2002.805411

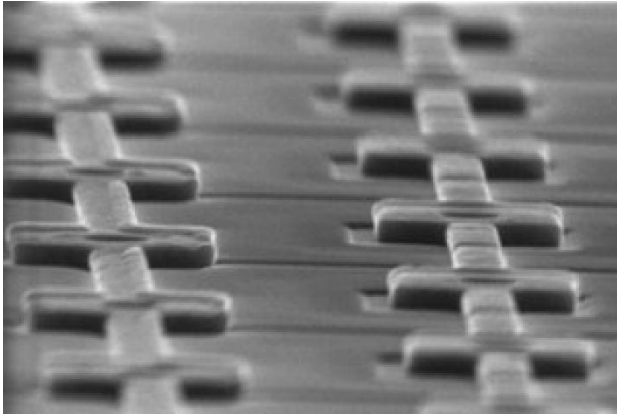


Fig. 1. Scanning electron microscopy image of silicon microdosimeter, showing array of planar pn junctions connected in parallel.

These studies involved the simultaneous measurement of amplitude (proportional to energy) and rise time of preamplifier signals for fully depleted p-i-n diodes. From this, a charged particle's energy, atomic number, and in some cases atomic mass could be determined. Theoretical models have shown this rise time to be related to the plasma decay time, the transit time of charge carriers, and to a lesser extent, the intrinsic rise time of the charge sensitive preamplifier [9].

Theoretical simulations of Bradley [12] looked at charge collection following 5 MeV alpha strikes for various strike locations on the microdosimeter. These studies indicated that the duration of the resulting current pulse increased with the distance of the ion strike from the  $n^+$  region, owing to larger transit times of charge carriers for diffusion versus drift. The aim of the current study is to correlate preamplifier rise time with ion strike position, and using suitable electronics, to discriminate charge collection events based on this timing information in order to preclude ion strikes outside the  $n^+$  region.

## II. HEAVY ION MICROPROBE AND IBIC SETUP

Experiments were performed with the heavy ion microprobe (HIMP) at the Australian Nuclear Science and Technology Organization (ANSTO), Lucas Heights, Australia. A detailed description of the microprobe facility is given by Siegle and Cohen [13]. The HIMP is situated on a 10 MV Tandem Van de Graaf accelerator equipped with two sputter ion sources and a charge exchange RF ion source allowing most elements of the periodic table to be accelerated. The desired ion species is accelerated to the required energy and steered to the microprobe beamline. Definition of the object to be demagnified is done using a pair of cylindrical, tungsten carbide  $x$  and  $y$  slits. The beam is then demagnified using a quadrupole triplet and raster scanned over the sample with a set of scanning coils positioned before the triplet (see Fig. 3).

The ion beam induced charge collection setup consists of a charge sensitive preamplifier (Amptek A250), mounted on a PC250 test board. A 10-pin electrical feed-through conveys the preamplifier power supply, device bias, test-pulse signal, and energy deposition signal to and from the target chamber. Calibration of the IBIC system is done using a fully depleted p-i-n

diode, of capacitance similar to the sample, and a 3 MeV proton beam.

For the present experiments, a 20 MeV  $C^{+3}$  beam was focussed to a spot size of  $1\ \mu\text{m}$  and the beam was scanned over an area of  $100 \times 100\ \mu\text{m}^2$ . The  $10\ \mu\text{m}$  SOI device was measured at a reverse bias of 10 V. The microprobe is equipped with a forward mounted CCD camera and microscope. Prior to performing the IBIC scan of the microdosimeter, the beam is raster scanned, with the same scan size as the IBIC scan, across a quartz crystal. The scan area, indicated by fluorescence of the quartz, is then marked out on an optical image acquired with the CCD camera. This enables the translation of scan coordinates generated by the data acquisition system to coordinates in the optical image. The microdosimeter array is then moved into the scan area, and into the field of view of the optical system, and the position of each  $n^+$  region in the IBIC scan area is noted.

## III. TIMING MEASUREMENTS

### A. Experimental Method

The first experiment involved measurement of the rise-time of the preamplifier signal as a function of the distance of the ion strike from the pn junction. The rise-time was measured with a technique similar to the one used by Pausch *et al.* [10] and is illustrated in the schematic of Fig. 3. The preamplifier output is passed to timing filter amplifiers with differentiation and integration time constants of  $\tau_{\text{int}} = 5\ \text{ns}$  and  $\tau_{\text{diff}} = 200\ \text{ns}$ . The differentiation produces a bipolar signal as illustrated in Fig. 3. It can be shown the zero-crossing time (referred to herein as  $T_{zc}$ ) of the resulting bipolar signal is a monotonic increasing function of the rise time [10] of the charge sensitive preamplifier. This in turn is related to the charge collection time. The bipolar signal is split and fed into two constant fraction discriminators (CFDs). One of these is operated in "rise-time compensation mode" for which the CFD produces a logic pulse after a time  $t = t_d / (1 - f)$  where  $t_d$  is the delay time on the CFD and  $f$  is the constant fraction, set at 0.2 for commercial CFDs. This time is independent of pulse height and rise-time.  $t_d$  was adjusted so as the logic pulse occurs just as the leading edge of the bipolar signal rises above the background noise. The second CFD is operated as a simple zero crossing discriminator, such that the CFD produces a logic pulse when the bipolar signal crosses zero (see Fig. 3). The constant fraction discriminator output pulses are used as start and stop signals for a time-to-amplitude converter. The output of this is fed into a channel of the microprobe data acquisition system along with the ion beam coordinates. During measurements a file of data triplets ( $T_{zc}, x, y$ ) is accrued and an event histogram may be formed. To correlate zero-crossing time with ion strike position, a window of the spectrum is selected and a two-dimensional (2-D) image of the number of events occurring at each pixel of the scan and lying within the window is formed (i.e.,  $N(T_{zc} + \Delta T_{zc}, x, y)$ ).

### B. Results and Discussion

Fig. 4 shows the total spectrum of  $T_{zc}$  events measured and is composed of two peaks. Fig. 5 shows the number of ion strikes registered at each pixel of the scan which lie within the given

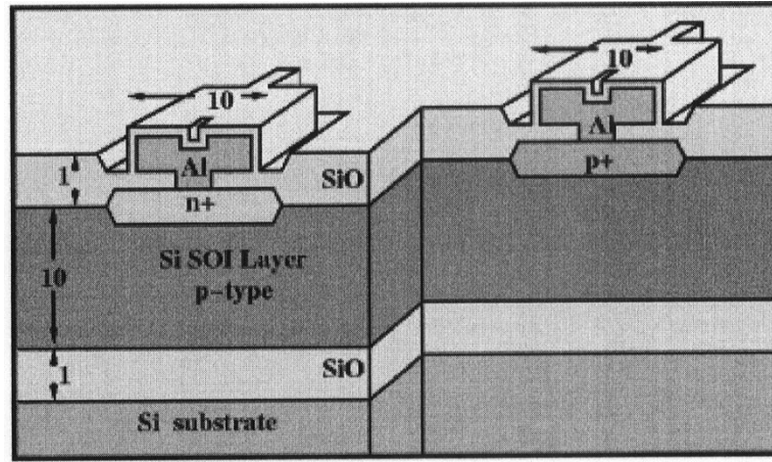


Fig. 2. Cross section of 10- $\mu\text{m}$  silicon on insulator device. All dimensions are in microns.

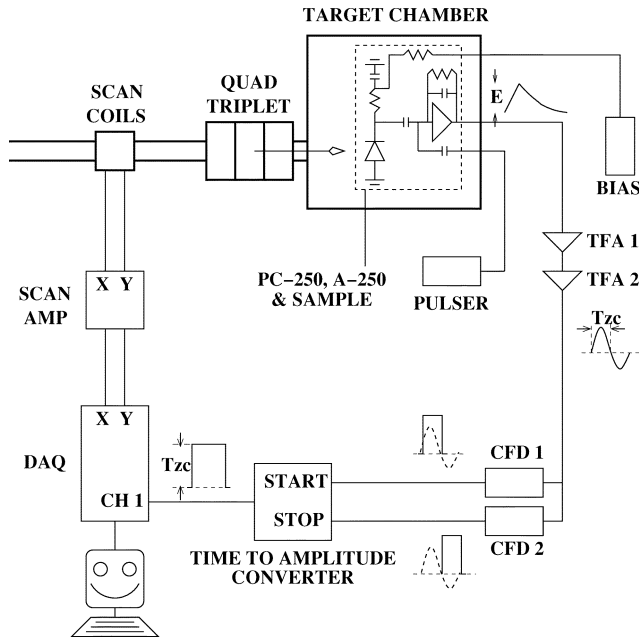


Fig. 3. Circuit diagram for zero-crossing time measurements of preamplifier output. TFA: Timing filter amplifier, CFD: constant fraction discriminator, DAQ: Data acquisition system. Voltage signals at various stages of the circuit are illustrated.

window of the  $T_{zc}$  spectrum of Fig. 4. The results clearly show the zero crossing time,  $T_{zc}$  and hence preamplifier rise-time increases as the distance of the ion strike from the  $n^+$  region increases. This is a direct result of the corresponding increase in charge collection time. The charge collection time depends upon the mechanisms of charge collection in the device. For ion strikes close to the pn junction, the motion of charge carriers is dominated by drift under the influence of the electric field of the depletion region and charge collection is rapid. As the ion strike moves further from the junction, the electric field magnitude decreases and charge collection is dominated by the diffusion of charge carriers. The charge carriers must first diffuse some distance to the depletion region prior to being collected by the electric field. As the ion strike moves further from the junction, this diffusion distance increases, resulting in longer collection times. From the results obtained, ion strikes are confined to the

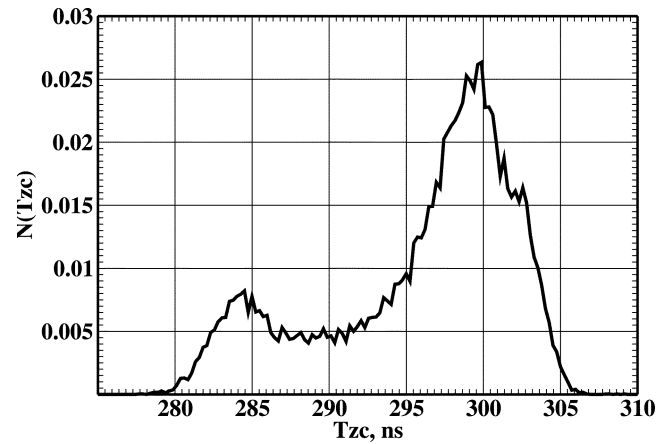


Fig. 4. Total zero crossing time spectrum obtained with 20 MeV carbon-12 ions incident on the 10- $\mu\text{m}$  SOI device.

geometrical boundaries of the  $10 \times 10 \mu\text{m}$   $n^+$  region for zero crossing times,  $T_{zc} \leq 284$  ns.

#### IV. PULSE-SHAPE DISCRIMINATION

##### A. Experimental Method

To preclude nonjunction strikes, a window incorporating zero-crossing times,  $0 \text{ ns} < T_{zc} \leq 284 \text{ ns}$  was set on the single channel analyzer of the time to amplitude converter (see Fig. 6). The single channel analyzer provides a logic pulse which is used as the “enable” signal of a linear gate, through which the output of the spectroscopy amplifier is passed. The function of the spectroscopy amplifier is to shape the signal from the charge sensitive preamplifier to provide a pulse suitable for the multi channel analyzer of the data acquisition system and with a pulse height proportional to energy deposition.

Using this circuit, only energy events corresponding to  $T_{zc} < 284 \text{ ns}$  would pass through the linear gate and be registered by the data acquisition system along with the beam coordinates. Energy deposition event spectra were acquired with and without the pulse-shape discrimination system. Additionally, a 2-D image of the number of events occurring at each pixel of the scan with the PSD system (i.e.,  $N(x, y)$ ) was constructed.

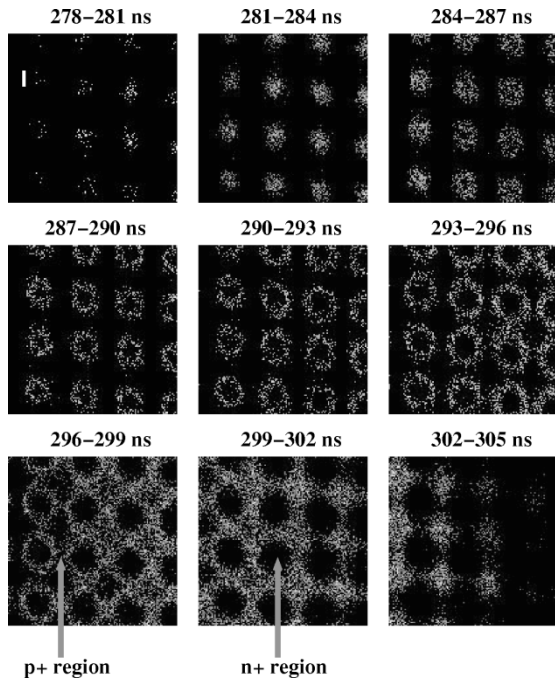


Fig. 5.  $N(T + \Delta T_{zc}, x, y)$  maps for  $T_{zc}$  windows of the spectrum of Fig. 4. The white bar in the first map indicates a distance of  $10\text{-}\mu\text{m}$ .

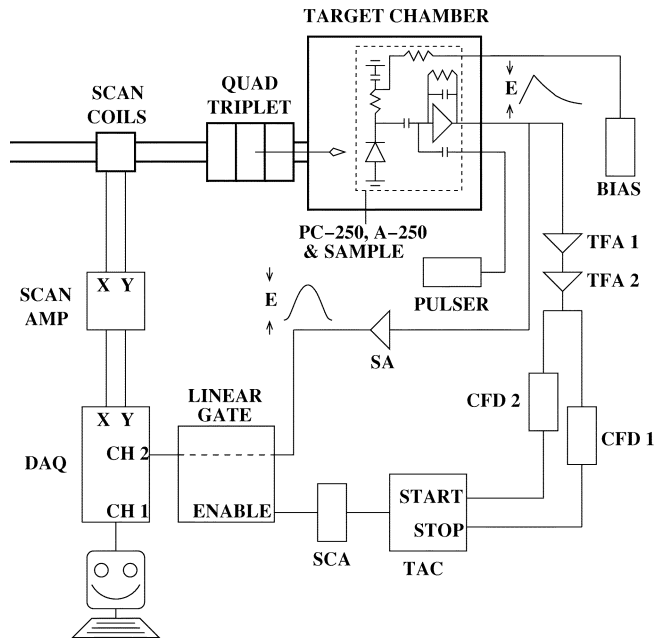


Fig. 6. Circuit diagram for system used to gate the energy signal with a pulse-shape discrimination technique. SCA: single channel analyzer, SA: Spectroscopy amplifier, TAC: Time-to-amplitude converter. Signals at charge sensitive preamplifier and spectroscopy amplifier outputs are shown.

### B. Results and Discussion

Fig. 7 shows the total energy spectrum before and after the pulse shape discrimination technique is implemented. The low-energy component of the spectrum is drastically reduced and the energy deposition spectrum is close to Gaussian. Fig. 8 confirms the position of all ion strikes to be within the geometrical boundaries of the  $n^+$  region.

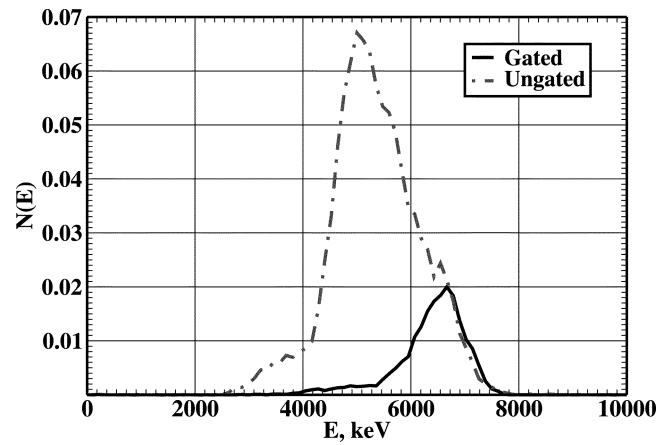


Fig. 7. Charge collection spectra obtained with (solid line) and without (broken line) pulse-shape discrimination.

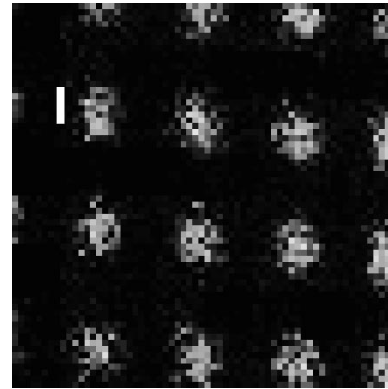


Fig. 8. Intensity map of ion strikes for window spanning entire gated energy deposition spectrum (i.e.,  $N(x, y)$ ).

### V. CONCLUSION

The timing properties of a silicon-on-insulator microdosimeter for medical and space applications have been studied using an ion microprobe. This study showed that the zero crossing time  $T_{zc}$  parameter, closely related to charge collection time, increased as a function of radial distance of ion strike from each pn junction. These timing properties were used to implement a pulse shape discrimination technique to render the microdosimeter insensitive to ion strikes outside the  $n^+$  region.

The effective microdosimeter sensitive volume is cubic with dimensions  $10 \times 10 \times 10 \mu\text{m}^3$ , the energy deposition event spectrum is close to Gaussian for a mono-energetic source. This is expected to improve detector performance in a clinical environment by removing artifacts in the energy deposition event spectrum created by events suffering high recombination (non junction strikes). As the sensitive volume is closer to a cubic shape the variance in the distribution of chord lengths will be reduced. Also as charge collection is dominated by drift of charge carriers there is expected to be a decreased sensitivity to radiation damage.

The charge collection time is dependent upon the plasma decay time as well as the charge transit time. The plasma decay time is believed to be dependent upon ion LET. Further studies with the ANSTO microprobe are planned to investigate

the influence of ion LET on the timing properties of the microdosimeter over the LET range relevant to hadron therapy (1 – 1000 keV/ $\mu$ m).

Future studies will also investigate the effectiveness of this technique in minimizing distortions of lineal energy spectra in realistic densely ionizing radiation fields of hadron therapy.

#### ACKNOWLEDGMENT

The authors would like to acknowledge the efforts of the Accelerator Operations Team, Physics Division, ANSTO and the technical staff of the Department of Engineering Physics, University of Wollongong. Thanks is also due to the Australian Institute of Nuclear Science and Engineering for their ongoing support.

#### REFERENCES

- [1] H. Rossi and M. Zaider, *Microdosimetry and its Applications*. Berlin: Springer-Verlag, 1996.
- [2] P. D. Bradley, A. B. Rosenfeld, and M. Zaider, "Solid state microdosimetry," *Nucl. Instrum. Methods Phys. Res. B*, vol. 184, pp. 135–157, 2001.
- [3] L. Z. Scheick, P. J. McNulty, and D. R. Roth, "Measurement of the effective sensitive volume of FAMOS cells of an ultraviolet erasable programmable read-only memory," *IEEE Trans. Nucl. Sci.*, vol. 47, pp. 2428–2434, 2000.
- [4] D. R. Roth, P. J. McNulty, W. J. Beauvais, R. A. Read, and E. G. Stassinopoulos, "Solid-state microdosimeter for radiation monitoring in spacecraft and avionics," *IEEE Trans. Nucl. Sci.*, vol. 41, pp. 2118–2124, 1994.
- [5] P. D. Bradley, A. B. Rosenfeld, B. J. Allen, J. Corderre, and J. Capela, "Performance of silicon microdosimetry detectors in boron neutron capture therapy," *Radiation Res.*, vol. 151, pp. 235–243, 1999.
- [6] A. B. Rosenfeld, P. D. Bradley, I. Cornelius, G. I. Kaplan, B. J. Allen, J. B. Flanz, M. Goitein, A. Van Meerbeeck, J. Schubert, J. Bailey, Y. Tabkade, A. Maruhashi, and Y. Hayakawa, "New silicon detector for microdosimetry applications in proton therapy," *IEEE Trans. Nucl. Sci.*, vol. 47, pp. 1386–1394, Aug. 2000.
- [7] P. D. Bradley, A. B. Rosenfeld, K. K. Lee, D. Jamieson, and S. Satoh, "Charge collection and radiation hardness of a SOI microdosimeter for space and medical applications," *IEEE Trans. Nucl. Sci.*, vol. 45, pp. 2700–2710, Dec. 1998.
- [8] I. Cornelius, R. Siegele, A. Rosenfeld, and D. Cohen, "Ion beam induced charge collection imaging of a silicon microdosimeter using a heavy ion microprobe," *Nucl. Instrum. Methods Phys. Res. B*, vol. 190, pp. 335–338, 2001.
- [9] J. B. A. England, G. M. Field, and T. R. Ophel, "Z-identification of charged particles by signal risetime in silicon surface barrier detectors," *Nucl. Instrum. Methods Phys. Res. A*, vol. 280, pp. 291–298, 1989.
- [10] G. Pausch, H. G. Ortlepp, W. Böhne, H. Grawe, D. Hilscher, M. Moszynski, D. Wolski, R. Schubert, D. de Angelis, and M. de Poli, "Identification of light charged particles and heavy ions in silicon detectors by means of pulse-shape discrimination," *IEEE Trans. Nucl. Sci.*, vol. 43, pp. 1097–1011, June 1996.
- [11] C. A. J. Ammerlaan, R. F. Rumphorst, and L. A. C. Koerts, "Particle identification by pulse shape discrimination in the p-i-n type semiconductor detector," *Nucl. Instrum. Methods*, vol. 22, pp. 189–200, 1963.
- [12] P. D. Bradley, "The Development of a Novel Silicon Microdosimeter for High LET Radiation Therapy," Ph.D. dissertation, Univ. Wollongong, Wollongong, Australia, 2000.
- [13] R. Siegele, D. D. Cohen, and N. Dytlewski, "The ANSTO high energy heavy ion microprobe," *Nucl. Instrum. Methods Phys. Res. B*, vol. 158, pp. 31–38, 1999.